

Two Dimensional Microwave Imaging Using a Divide and Unite Algorithm

Disha Shur¹, K. Yaswanth², and Uday K. Khankhoje²

¹Indian Institute of Engineering Science and Technology, Shibpur, India

²Indian Institute of Technology, Madras, India

Abstract— Quantitative microwave imaging using inverse scattering is a promising technique for biomedical imaging. Given the ill-posed nature of the inverse problem, the use of efficient regularization techniques is essential in order to come up with meaningful solutions to the imaging problem. In this paper, we propose a novel regularization technique that is based on an iterative divide-and-unite algorithm of the imaged domain. Multi-scaling procedures have been proposed earlier, where the object domain is iteratively divided based on heuristic criteria. We take a different route, where, starting from a single coarse pixel, the domain is divided into finer pixels based on heterogeneity in the gradient of the cost function. An inexpensive algebraic reconstruction technique is then applied to estimate the values of the finer pixels. Subsequently, an unite step is performed to combine pixels with similar values of dielectric contrast. The power of this method is that it keeps the number of reconstructed pixels at a minimum and allows for nonlocal pixels, as also seen in level-set based reconstructions. Implementation of the algorithm shows a significant reduction in converging time, the cost function and the total shape error.

1. INTRODUCTION

This paper deals with a quantitative reconstruction of dielectric scatterers using inverse microwave imaging which is potentially equipped to address problems in the field of nondestructive testing and evaluation, and medical imaging [1]. The general approach in this regard involves solving the inverse problem using the available optimization techniques [2–5] illustration of the problem setup in Section 2. The effectiveness of the algorithm is depicted in the form of various numerical simulations in Section 4, which is followed by significant observations and future work in this regard in Section 5.

2. PROBLEM FORMULATION

The domain D , in Fig. 1, is illuminated by a single wavelength, λ , by one of the transceivers from the boundary S and the scattered field is collected by the remaining ones. This procedure is repeated for each of the shown transceivers with one of them acting as transmitters and the rest acting as receivers. The relation between the scatterer profile and the scattered field is governed by the following equation [8]:

$$E_j^{scat}(\vec{r}) = E_j(\vec{r}) - E_j^{inc}(\vec{r}) = k_b^2 \iint_D G(\vec{r} - \vec{r}') \chi(\vec{r}') E_j(\vec{r}') d^2 \vec{r}' \quad (1)$$

where $\chi(\vec{r}') = \epsilon_r(\vec{r}') - 1$, $\chi(\vec{r}')$ is the contrast and $\epsilon_r(\vec{r}')$ is the relative permittivity at position \vec{r}' , $E_j^{scat}(\vec{r})$, $E_j(\vec{r})$ and $E_j^{inc}(\vec{r})$ are the scattered field, total field and the incident field respectively due to the j th transmitter at position \vec{r} and G is the 2D Green's function.

As for reconstruction of the scatterer profile using the obtained scattered fields, the domain D is discretized according to Richmond's procedure [9] into a mesh of $p \times p$ pixels such that the unknowns, the contrast, $\chi(\vec{r}')$ and the total electric field, $E_j(\vec{r})$, are constant inside each pixel. Post-discretization, (1) can be written as follows:

$$G_D \mathbf{x} = g_D \quad \text{for } \vec{r}, \vec{r}' \in D \quad (2a)$$

$$G_S \mathbf{x} = g_S \quad \text{for } \vec{r} \in S, \vec{r}' \in D \quad (2b)$$

where g_D and g_S are functions of the incident and the scattered field and G_D and G_S are functions of the total electric field in D and S respectively. At each step the values for \mathbf{x} are obtained by minimizing the following equation:

$$\phi = \|G_S \mathbf{x} - \mathcal{J}\|_2^2 \quad (3)$$

where \mathcal{J} is the measured scattered field, and \mathbf{x} is the vector holding the contrast values for pixels in the investigation domain.

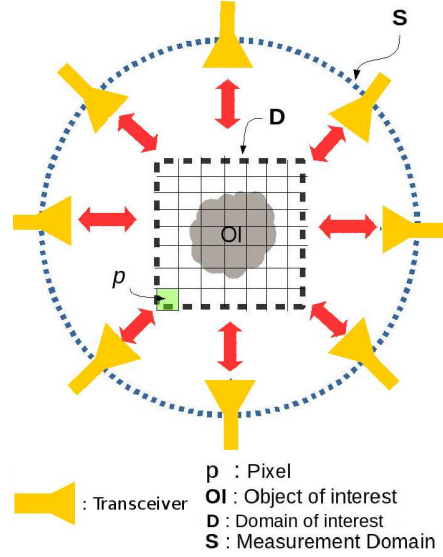


Figure 1: Problem setup.

3. DUC ALGORITHM

The algorithm is guided by the fact that if the entire domain D is divided into super-pixels based on their contrast value (where a super-pixel implies a sub-domain $\tilde{\mathbf{x}} \in D$, connected or disconnected, having the same contrast value), there will be only as many super-pixels as many different contrast values are there within D .

A coarse mesh is defined which holds only as many super-pixels as required by the heterogeneity of the contrast values within D , denoted by \mathbf{x} as the fine mesh. Each super-pixel is a linear combination of all the pixels within the same cluster, where the threshold for similarity has been predetermined. The following equation is to be followed for implementing the same:

$$k_{m,n} = \sum_{i=1}^{p \times p} a_{m,i}^{(n)} x_{m,i} \quad (4)$$

where $k_{m,n}$ is the contrast of the n th super-pixel in coarse mesh, $\tilde{\mathbf{x}}_m$, at the m th iteration, and $x_{m,i}$ is the contrast of the i th pixel in the fine mesh. $p \times p$ is the number of elements in the fine mesh \mathbf{x}_m , and $a_{m,i}^{(n)}$ is the (n, i) th element of a transformation matrix T , such that

$$a_{m,i}^{(n)} = \begin{cases} \frac{1}{\text{number of } x_i \in k_{m,n}} & \text{if } x_i \in k_{m,n} \\ 0 & \text{otherwise} \end{cases} \quad (5a)$$

where the transformation matrix, T_m , that controls the evolution of the coarse mesh, $\tilde{\mathbf{x}}_m$ at the m th step, is defined as

$$T_m \mathbf{x}_m = \tilde{\mathbf{x}}_m \quad (5b)$$

T_m at m th iteration is set by predetermined conditions as will be shown in the following sections.

Before the algorithm is outlined, its significant components are discussed. They can be divided into three major blocks to be followed sequentially: division, reconstruction and unification. It starts with a coarse mesh with just one super-pixel and a corresponding fine mesh such that

$$k_{1,1} = \sum_{i=1}^{p \times p} a_{1,i} x_{1,i}$$

where $a_{1,i} = \frac{1}{p^2}$.

All the equations mentioned henceforth are to be followed at each iteration m .

3.1. Division

The breakdown of each super-pixel in the coarse mesh, $\tilde{\mathbf{x}}$, is determined by the gradient of cost function, $\nabla\phi$ at each $x_i \in \mathbf{x}^*$, such that

$$\nabla_{\mathbf{x}^*}\phi = G_S^\dagger(G_S\mathbf{x}^* - \mathcal{J}) \quad (6a)$$

where A^\dagger and A^* imply conjugate transpose and conjugate of A , respectively.

Now, each $x_i^{(n)}$, where n is the index of the super-pixel k_n to which it belongs, is considered for separation from its super-pixel based on the conditions outlined below:

For $n = 1, 2, \dots, \ell$, $\alpha_n = 0.3 \times \max |x_j^{(n)} - x_k^{(n)}|$, where ℓ is the number of super-pixels in $\tilde{\mathbf{x}}$ and α_n is the threshold for division for the n th super-pixel.

$$\text{For } n = 1, 2, \dots, \ell, \quad |\nabla_{x_j}\phi^{(n)} - \nabla_{x_k}\phi^{(n)}| > \alpha_n \quad (6b)$$

and

$$\max(\nabla_{x_j}\phi^{(n)}, \nabla_{x_k}\phi^{(n)}) > \eta_d \quad (6c)$$

where $\nabla_{x_i}\phi^{(n)}$ is the gradient at i th pixel of \mathbf{x}^* belonging to the n th pixel of $\tilde{\mathbf{x}}$ and η_d is an empirically decided threshold which stays constant across iterations and mostly depends on the reconstruction algorithm used. A super-pixel k_n is considered for division if its constituent pixels $x_i^{(n)}$ satisfy the above two conditions. Therefore, new super-pixels are defined which are comprised of the separated pixels and $a_i^{(n)}$ is altered according to the new super-pixels $k_n \in \tilde{\mathbf{x}}$ and its constituent pixels $x^{(n)} \in \mathbf{x}$.

3.2. Reconstruction

ϕ in Equation (4) is minimized here, using Algebraic reconstruction technique (ART) [2], with respect to the super-pixels $k_{m,n} \in \tilde{\mathbf{x}}_m$, such that,

$$k_{m+1,n} = \left[k_{m+1,n} \in \tilde{\mathbf{x}}_{m+1} : \min_{\tilde{\mathbf{x}}} \|(G_S \times T^{-1}) \tilde{\mathbf{x}} - \mathcal{J}\|_2^2 \right] \quad (7)$$

3.3. Unification

For further reduction of the effective domain under investigation, super-pixels in the coarse mesh are merged according to their reconstructed values. The threshold for unite, β is defined as

$$\beta = \eta_u \times [\max(\tilde{\mathbf{x}}) - \min(\tilde{\mathbf{x}})] \quad (8a)$$

where η_u stays constant across iterations and can be kept anywhere between 10%–40% (empirically determined).

A pair of super-pixel is considered for unification, if

$$|k_j - k_k| < \beta \quad \forall \quad k_n \in \tilde{\mathbf{x}} \quad (8b)$$

Consequently, the j th row and the k th row of the transformation matrix T are modified according to the freshly calculated weight, $a_i^{(n)}$ as per Equation (5).

3.4. Convergence

Convergence of the algorithm is determined by comparing values of ϕ for two consecutive iterations.

$$\frac{|\phi_{m+1} - \phi_m|}{\phi_m} < \epsilon \quad (9)$$

where ϵ has been set at 10^{-3} .

The algorithm terminates if the above equation is satisfied or if a maximum number of iterations is reached, which is 100 in this case.

3.5. Algorithm

- i Initialization by Born Approximation [8]: $\chi = 0$ and $E = E_{inc}$
- ii Initialize G_S, G_D, \mathcal{J} and g_D : Equation (2)
- iii Compute ϕ_1 : Equation (3)
- iv Check for division:
 - Compute gradient: Equation (6)
 - Check for super-pixels that need division: Equations (6.1) and (6.2)
 - Modify T and update $\tilde{\mathbf{x}}$: Equations (5) and (5.1)
- v Reconstruction of $\tilde{\mathbf{x}}$ using ART and update \mathbf{x} : Equations (7) and (5a)
- vi Check for unification:
 - Check for super-pixels that need merging: Equation (8.1)
 - Modify T and update $\tilde{\mathbf{x}}$: Equations (5) and (5a)
- vii Update G_S, G_D and g_D , and solve forward problem: Equations (2) and (1)
- viii Compute ϕ : Equation (3)
- ix Check convergence: Equation (9)
 - If convergence achieved: **END**
 - Else: Proceed to Step (iv)

4. RESULTS

Various numerical simulations are presented below to validate the effectiveness of the proposed algorithm. The setup involves an object of size 1.2λ illuminated by 27 transmitters one by one on a radius of 3λ , and the scattered field due each transmitter is collected by 27 receivers at the

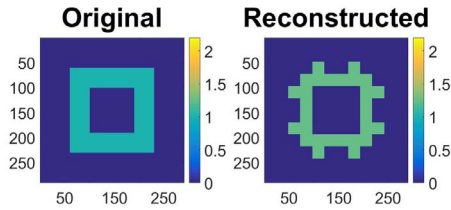


Figure 2: Contrast = 1, with DUC ($\eta_d = 0.07$ and $\eta_u = 0.1$).

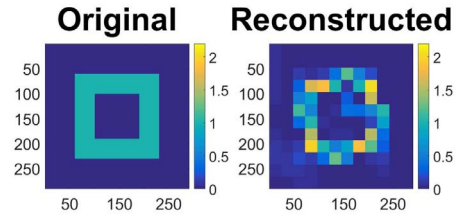


Figure 3: Contrast = 1, with ART.

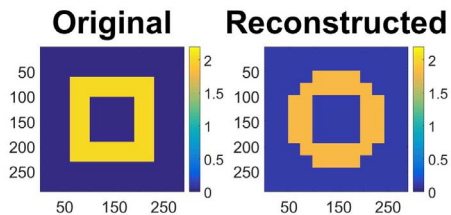


Figure 4: Contrast = 2, with DUC ($\eta_d = 0.5$ and $\eta_u = 0.4$).

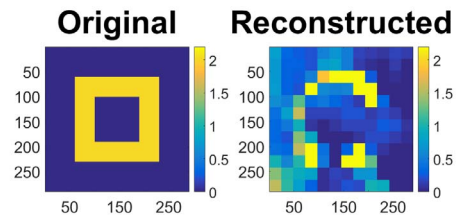


Figure 5: Contrast = 2, with ART.

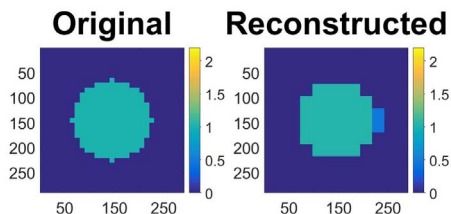


Figure 6: Contrast = 1, with DUC ($\eta_d = 0.15$ and $\eta_u = 0.17$).

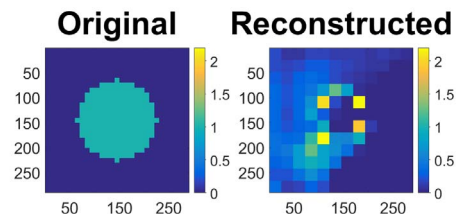


Figure 7: Contrast = 1, with ART.

same radius. First, the forward problem is solved for each object and then the generated scattered field is used to run the inverse problem and reconstruct the object. To avoid inverse crime, the discretization used for synthetic problem is $\frac{\lambda}{24}$ and that for inverse is $\frac{\lambda}{10}$.

Example 1: Here we have performed a noiseless reconstruction of a ring like object of outer and inner length $\frac{2\lambda}{3}$ and $\frac{\lambda}{3}$ respectively for a contrast value of 1 (Fig. 2) and 2 (Fig. 4). Fig. 3 (for a contrast of 1) and Fig. 5 (for a contrast of 2) show the reconstruction of the same object using only ART.

The following table shows the corresponding values of final cost function and total error.

Name	Cost function	Super-pixels	Total error (%)	Iterations	Time taken (seconds)
Contrast = 1, with DUC	0.1	2	10.1	30	30.6
Contrast = 1, with ART	0.2	144	11.8	60	73.6
Contrast = 2, with DUC	3.6	2	21.9	58	57.87
Contrast = 2, with ART	194	144	52.9	60	75.3

Example 2: We have attempted a noiseless reconstruction of a circular object of radius $\frac{\lambda}{3}$ centered at the origin for contrast values of 1 (Fig. 6) and 2 (Fig. 8). Fig. 7 (for a contrast of 1) and Fig. 9 (for a contrast of 2) show the reconstruction of the same object using only ART.

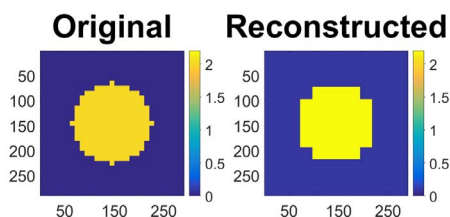


Figure 8: Contrast = 2, with DUC ($\eta_d = 0.5$ and $\eta_u = 0.3$).

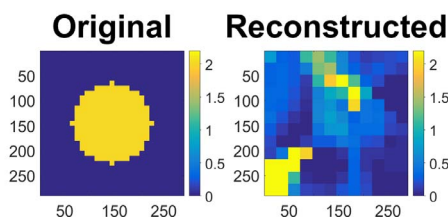


Figure 9: Contrast = 2, with ART.

The following table shows the corresponding values of final cost function and total error.

Name	Cost function	Super-pixels	Total error (%)	Iterations	Time taken (seconds)
Contrast = 1, with DUC	0.09	3	3.3	22	23
Contrast = 1, with ART	66.88	144	23.2	60	76.7
Contrast = 2, with DUC	1.8	2	10	49	49.7
Contrast = 2, with ART	232.8	144	63.1	60	73.7

Example 3: In this example, the original image consists of two semicircular rings of different radii with a contrast value of 1 (Fig. 10) and 2 (Fig. 11). Fig. 12 (for a contrast of 1) and Fig. 13 (for a contrast of 2) show the reconstruction of the same using only ART.

The following table shows the corresponding values of cost function and total error.

Name	Cost function	Super-pixels	Total error (%)	Iterations	Time taken (seconds)
Contrast = 1, with DUC	0.04	8	8.5	31	33.3
Contrast = 1, with ART	0.001	144	9.4	26	33.6
Contrast = 2, with DUC	5.23	5	18.23	46	48.43
Contrast = 2, with ART	140.6	144	31.5	60	76

Example 4: This example shows the performance of the algorithm for data corrupted by noise at an SNR value of 20 dB. Figs. 14 and 15 show the reconstruction of the above object for contrast values of 1 and 2 respectively.

The following table shows the corresponding values of cost function and total error for Figs. 14 and 15.

Example 5: This example shows the performance of the algorithm for data corrupted by noise. Figs. 16 and 17 show the reconstruction of a ring like object for a contrast value of 1 for noise levels of 20 dB and 40 dB respectively. Figs. 18 and 19 show the same reconstruction for a contrast value of 2.

The following table shows the corresponding values of cost function and total error.

Name	Cost function	Super-pixels	Total error (%)	Iterations	Time taken (seconds)
Contrast = 1, at 20 dB	0.7	4	7.9	20	21.8
Contrast = 2, at 20 dB	2.4	3	13.5	59	62.3

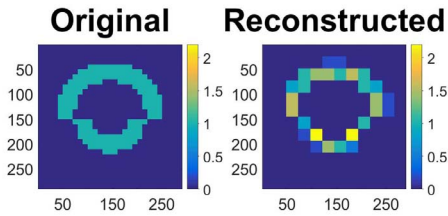


Figure 10: Contrast = 1, with DUC ($\eta_d = 0.05$ and $\eta_u = 0.05$).

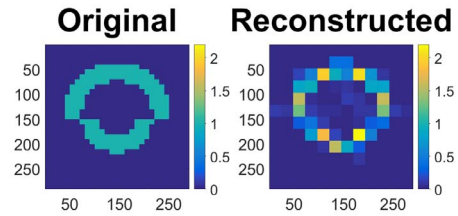


Figure 11: Contrast = 1, with ART.

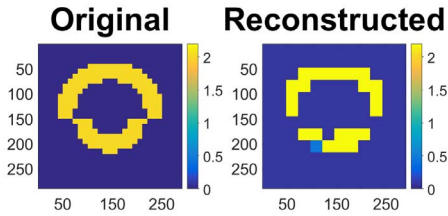


Figure 12: Contrast = 2, with DUC ($\eta_d = 0.5$ and $\eta_u = 0.05$).

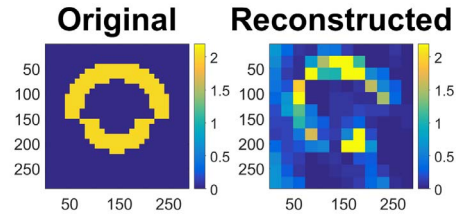


Figure 13: Contrast = 2, with ART.

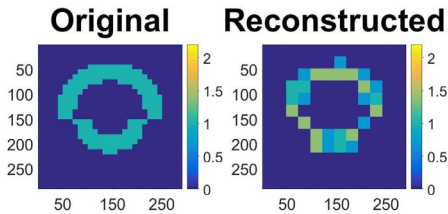


Figure 14: Contrast = 1, at 20 dB ($\eta_d = 0.3$ and $\eta_u = 0.1$).

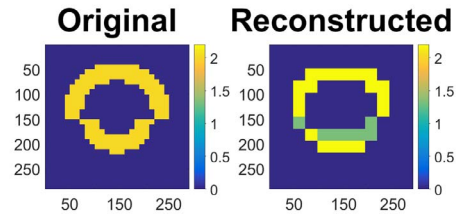


Figure 15: Contrast = 2, at 20 dB ($\eta_d = 0.32$ and $\eta_u = 0.1$).

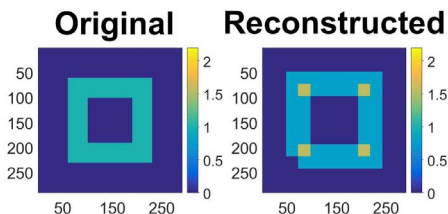


Figure 16: Contrast = 1, at 20 dB ($\eta_d = 0.45$ and $\eta_u = 0.1$).

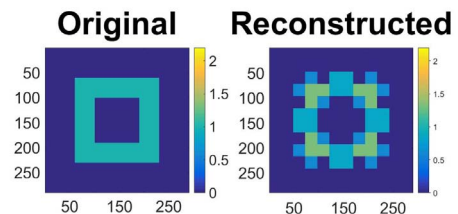


Figure 17: Contrast = 1, at 40 dB ($\eta_d = 0.07$ and $\eta_u = 0.1$).

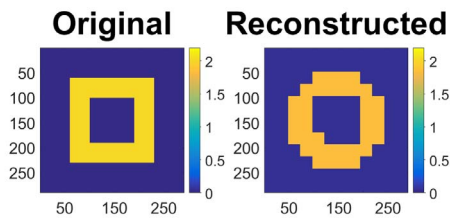


Figure 18: Contrast = 2, at 20 dB ($\eta_d = 0.6$ and $\eta_u = 0.2$).

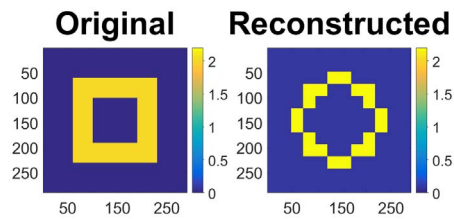


Figure 19: Contrast = 2, at 40 dB ($\eta_d = 0.73$ and $\eta_u = 0.2$).

Name	Cost function	Super-pixels	Total error (%)	Iterations	Time taken (seconds)
Contrast = 1, at 20 dB	2.7	3	11.5	11	12.5
Contrast = 1, at 40 dB	0.04	3	10.5	25	21.6
Contrast = 2, at 20 dB	2.8	2	19.7	19	20.9
Contrast = 2, at 40 dB	2.7	2	25.2	25	27.5

5. CONCLUSION

This paper proposes a new algorithm for efficient numerical reconstruction of dielectric scatterers. The basic idea is to represent the entire investigation domain with as less number of variables as possible, which makes this algorithm computationally efficient. Starting with one super-pixel, it iteratively modifies their population and the contribution of original pixels in each of them. Consequently, the optimization technique used with the cost function has to work with just the limited number of super-pixels and all the information contained in each of the original pixels of investigation domain is preserved. Additionally, it takes lesser execution time per iteration as compared to the other optimization algorithms. This algorithm takes care of the major limitation of overlooking scatterers as compared to the other existing algorithms which aim to reduce the domain size. Besides, as the entire investigation domain is represented by a few super-pixels, the reconstructed image obtained by implementing this algorithm is very sharp with precise values of contrast. Currently, the thresholds are extremely sensitive to noise and the optimization method used. An algorithm to make it automated is under progress. Besides, the upper limit of the contrast for which the algorithm works still remains to be verified.

Overall, the algorithm is guided by a novel approach for reducing the effective domain under computation and has shown promising results for scatterers in a wide range of contrast values and sizes.

REFERENCES

- Pastorino, M., "Medical and industrial applications of inverse scattering based microwave imaging techniques," *IEEE International Workshop on Imaging Systems and Techniques, 2008, IST 2008*, 1558–2809, Crete, Greece, September 2008.
- Yaswanth, K., S. Bhattacharya, and U. K. Khankhoje, "Algebraic reconstruction techniques for inverse imaging," *2016 International Conference on Electromagnetics in Advanced Applications (ICEAA)*, Cairns, Australia, September 2016.
- Harada, H., D. J. N. Wall, T. Takenaka, and M. Tanaka, "Conjugate gradient method applied to inverse scattering problem," *IEEE Transactions on Antennas and Propagation*, Vol. 43, No. 8, 784–792, 1995.
- Garnero, L., et al., "Microwave imaging-complex permittivity reconstruction-by simulated annealing," *IEEE Transactions on Antennas and Propagation*, Vol. 39, No. 11, 1801–1807, 1991.
- Pastorino, M., "Stochastic optimization methods applied to microwave imaging: A review," *IEEE Transactions on Antennas and Propagation*, Vol. 55, No. 3, 538–548, 2007.
- Caorsi, S., et al., "A new methodology based on an iterative multiscale for microwave imaging," *IEEE Transactions on Microwave Theory and Techniques*, Vol. 51, No. 4, 1162–1173, 2003.
- Liu, K. and J. Zou, "A multilevel sampling algorithm for locating inhomogeneous media," *Inverse Problems*, Vol. 29, 2013.

8. Wang, Y. M. and W. C. Chew, “An iterative solution of the two-dimensional electromagnetic inverse scattering problem,” *International Journal of Imaging Systems and Technology*, Vol. 1, No. 1, 100–108, 1989.
9. Richmond, J., “Scattering by a dielectric cylinder of arbitrary cross section shape,” *IEEE Transactions on Antennas and Propagation*, Vol. 13, No. 3, 334–341, 1965.